Alena Kohoutová
kohoutova@jinr.ru

# Simulation of a cryogenic gas stopping cell designed to study physical and chemical properties of superheavy elements

Joint Institute of Nuclear Research
Univerzita Palackého v Olomouci

AYSS 2023

Department of Experimental Physics

# Outline

- 1 Purpose
- 2 Cryogenic Gas Stopping Cell Setup
- 3 MR-TOF Setup
- 4 Stopping Efficiency Simulation of Cryogenic Gas Stopping Cell
- 5 Time of Flight Simulation of Cryogenic Gas Stopping Cell
- 6 Results
- 7 Conclusion

# 1 Purpose

- Choosing the optimal parameters for real experiment
- Stopping efficiency, TOF - Impossible to measure online, directly (short time of life)
- Need for theoretical simulations
- 1st part of simulations gave interval of optimal parameters – interval is then tested by 2nd part of simulations

# 2 Cryogenic Gas Stopping Cell Experimental Setup

**FLNR JINR DC-280 cyclotron complex (Super Heavy Element factory)**

**Experimental Hall**

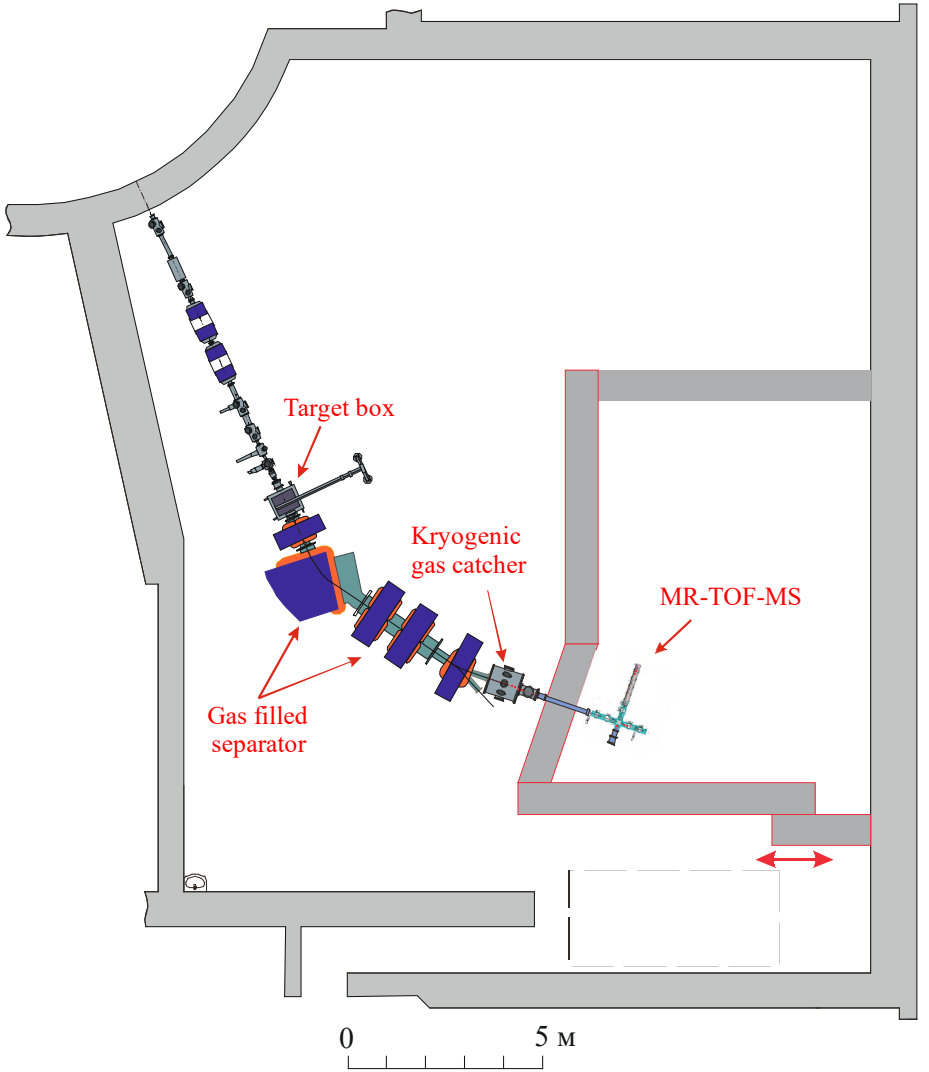

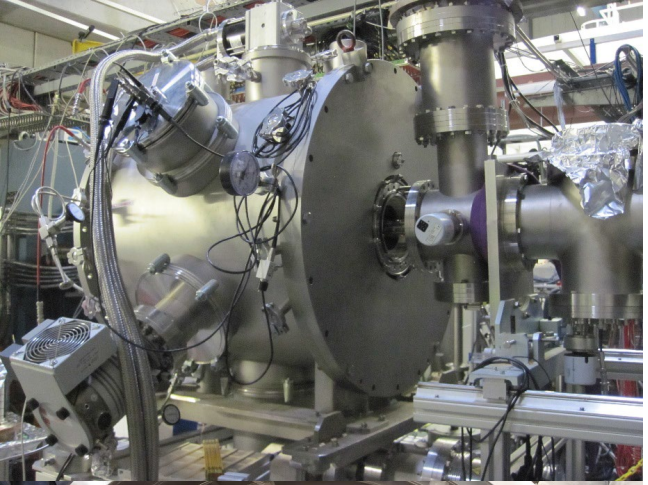

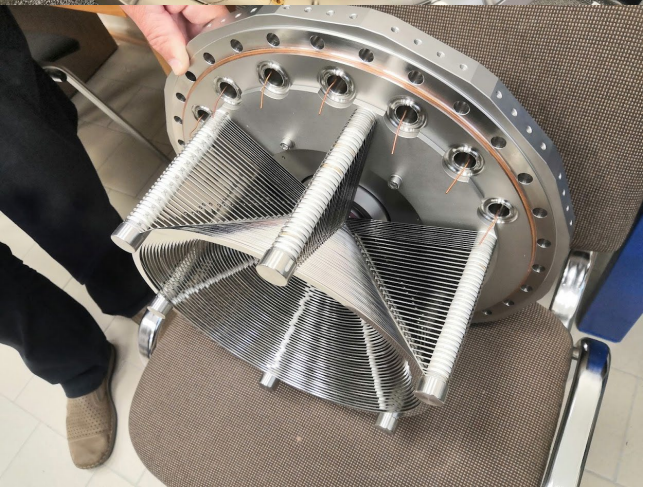

# 2 Cryogenic Gas Stopping Cell

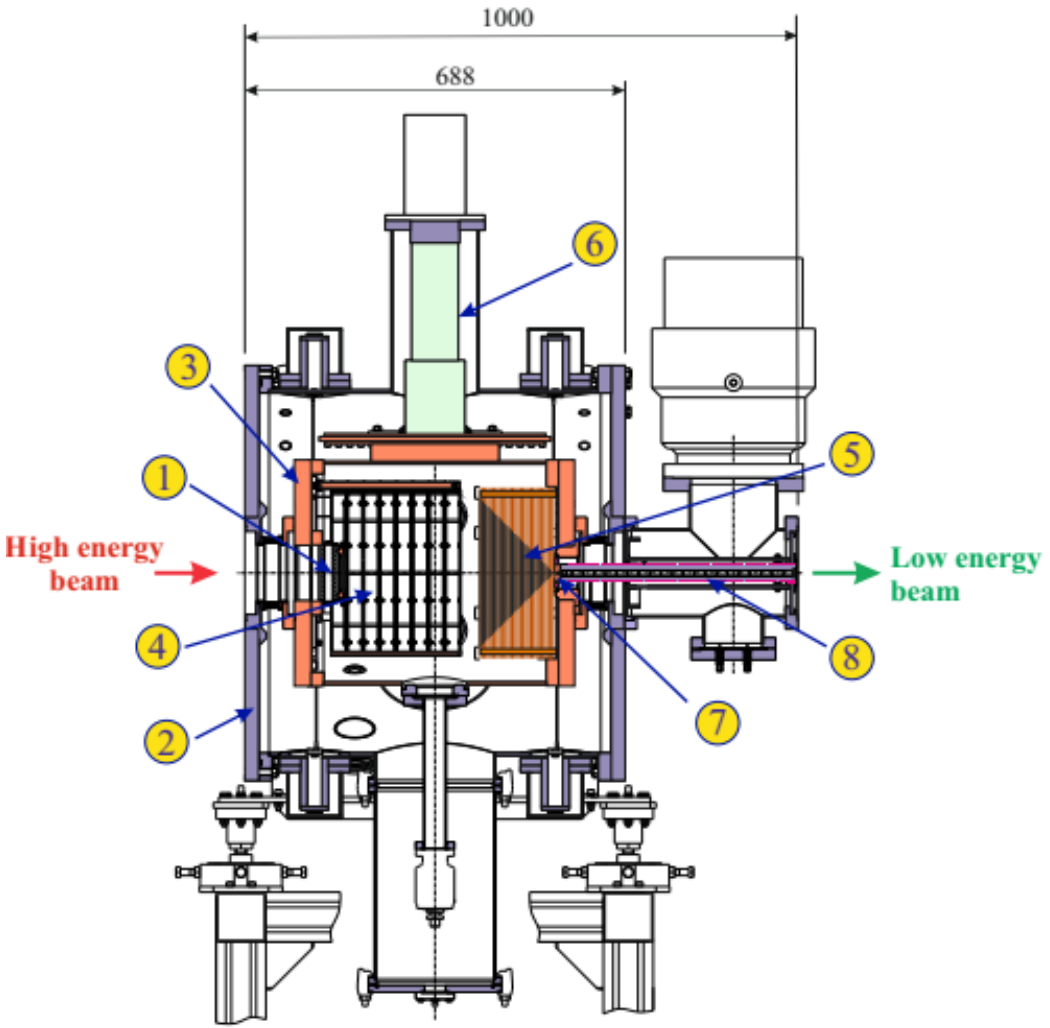


General view of a cryogenic gas ion trap. Positions in the figure:

1 - entrance window;
2 - outer warm vacuum shell;
3 - inner cold chamber;
4 - cylindrical electrodes of a constant electric field;
5 - radio frequency multi-electrode cone;
6 - the head part of the cryo-refrigerator;
7 - supersonic nozzle;
8 - transport radio frequency quadrupole.

# 3 Multiple-Reflection Time-of-Flight Spectrometer (MR-TOF-MS)

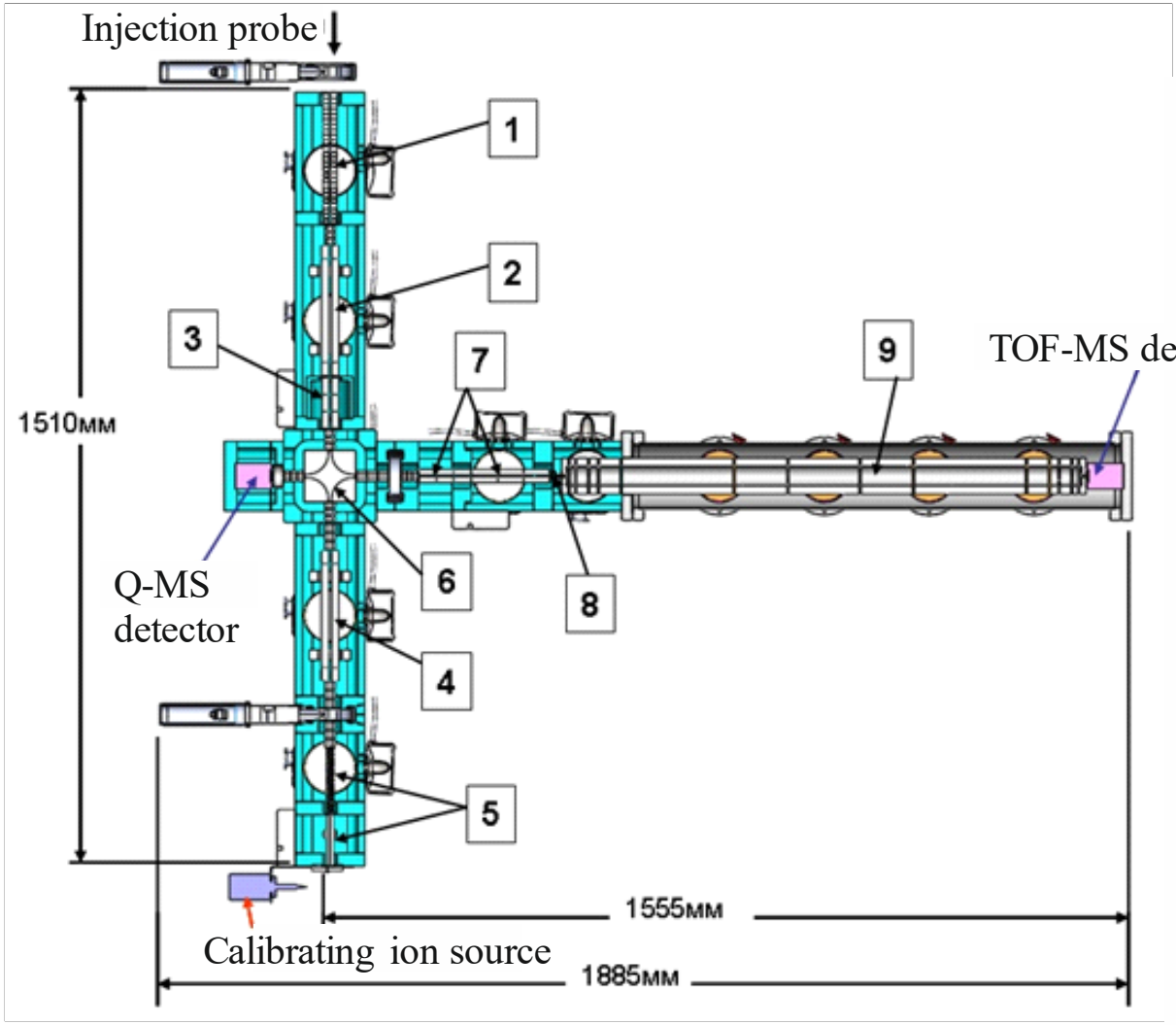


Analytical part of a multi-reflection time-of-flight mass spectrometer. The main nodes:

1 - collision induced dissociation cell;
2 - quadrupole RF filter of the sample;
3 - radio frequency trap of the sample channel;
4 - quadrupole radio-frequency filter of the calibrant;
5 - transporting system of the calibrant;
6 - quadrupole switchyard;
7 - channel for preparation and pulse extraction of ions;
8 - accelerating-transporting channel;
9 - time-of-flight analyzer.

# Stopping efficiency and TOF simulations for $^{182}$Hg and $^{203}$Rn isotopes, products with the maximal yields from reactions $^{40}$Ar+$^{144}$Sm→$^{184}$Hg* and $^{40}$Ar+$^{166}$Er→$^{206}$Rn*

- Simulations were performed for isotopes $^{182}$Hg and $^{203}$Rn and thickness of entrance window 3 μm and 4 μm, respectively.
- **GC_TRIM_Simulation** (directly connected to SRIM) software produces files:
  - Performs: simulations of **stopping efficiency** for particles in active volume of gas in CGSC
  - **RANGE_3D.txt** – coordinates in 3D of all, lost and stopped particles in active volume of helium gas, model of "cloud" can be reconstructed from it in origin software
  - **XYZ_position_file.xyz** – coordinates in 3D of lost and stopped particles in active volume of helium gas, is used for simulations of TOF by GasCellDynamic software in next step
- **GasCellDynamic** (in root framework, based on SIMION, Geant4 and COMSOL)
  - Performs **TOF** simulations by direct use of XYZ_position_file.xyz file (gained after simulation by GC-TRIM_Simulation)
  - Outputs:
    - **Info.txt** – information about simulation from interface of software (from histogram part)
    - **TOF** copied from interface of software-for TOF **histogram** created in origin software
- **Analysis**
  - **Origin** – histogram of TOF, Gauss fit, mean value of TOF, SD (standard deviation), variation
  - **Excel** – table of mean value of TOF, SD, variation
  - **Origin** – graphs of dependency of TOF mean value, SD, variation

# 4 Stopping Efficiency Simulation of Cryogenic Gas Stopping Cell

- **1st part of simulations**
- Energy loss of beam particles in chamber filled by buffer-gas (helium) is proportional to stopping material electron **density** (so also buffer-gas **pressure**).
- **Stopping efficiency**
- **Given by** fraction of $n_{stopped}$ stopped ions and the incoming ions $n_{inc}$ that lost their entire kinetic energy within the active gas volume of the Cryogenic Gas Stopping Cell (CGSC) :

$$\varepsilon_{stop} = \frac{n_{stopped}}{n_{inc} \cdot \varepsilon_{geom}}$$

- **Conditioned by** the kinetic energy of the incident EVR, the entrance window foil type and thickness and the buffer-gas type and density of the CGSC (only ions stopped within the active gas volume of the CGSC can be extracted)
- cannot be tested on-line - **relies on simulations**, our **internal software** based on SRIM is used
- **WHY? –** finding reactions, width of entrance window and pressure of buffer-gas optimal for real experiment (precious and expensive experimental time)

Simulations performed:

- $^{40}Ar + ^{144}Sm \rightarrow ^{184\text{-xn}}Hg$
- $^{40}Ar + ^{166}Er \rightarrow ^{206\text{-xn}}Rn$
- $^{48}Ca + ^{242}Pu \rightarrow ^{290\text{-xn}}Fl$
- $^{48}Ca + ^{208}Pb \rightarrow ^{256\text{-xn}}No$
- $^{48}Ca + ^{209}Bi \rightarrow ^{257\text{-xn}}Lr$

# 4 Stopping Efficiency Simulations

- **1st part** of simulations
- Performed by **internal software** created in Root framework based on software SRIM
- Capture coordinates of exact position of **stopped and lost particles**
- Calculate stopping efficiency
- Creates File of coordinates of exact position of stopped and lost particles
- Only stopped particles can be extracted

# 4 Stopped particles in CGSC

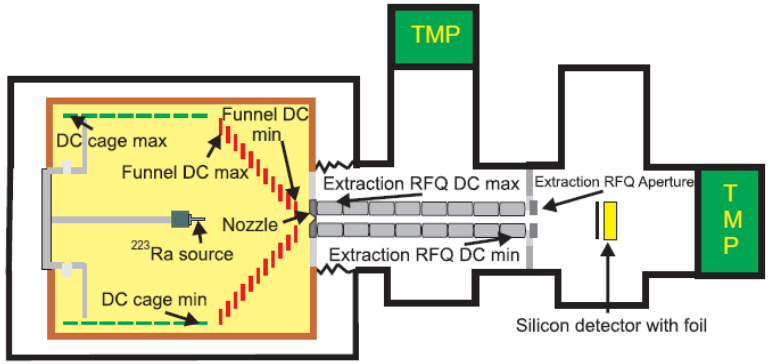


182Hg 50 mbar 4 μm, projection into y axis, plane perpendicular to entrance window

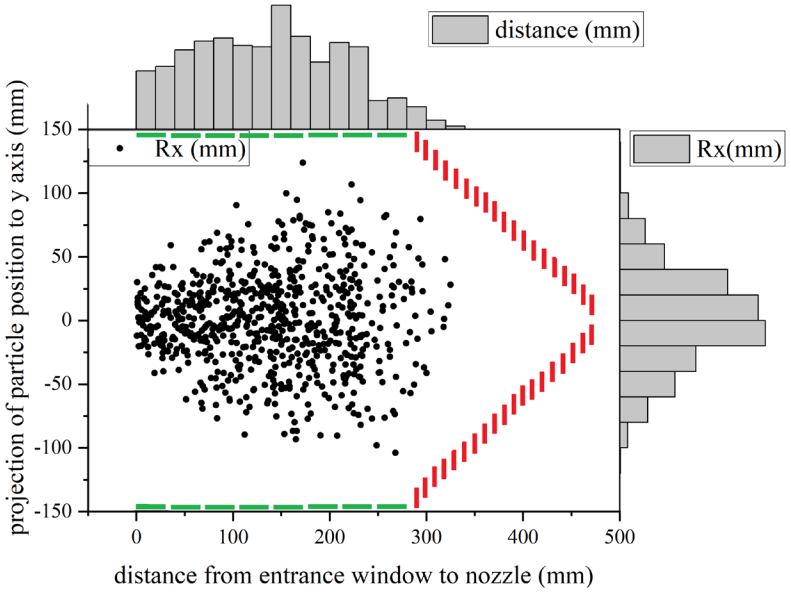


182Hg 50 mbar 4 μm, projection into plane paralel with entrance window

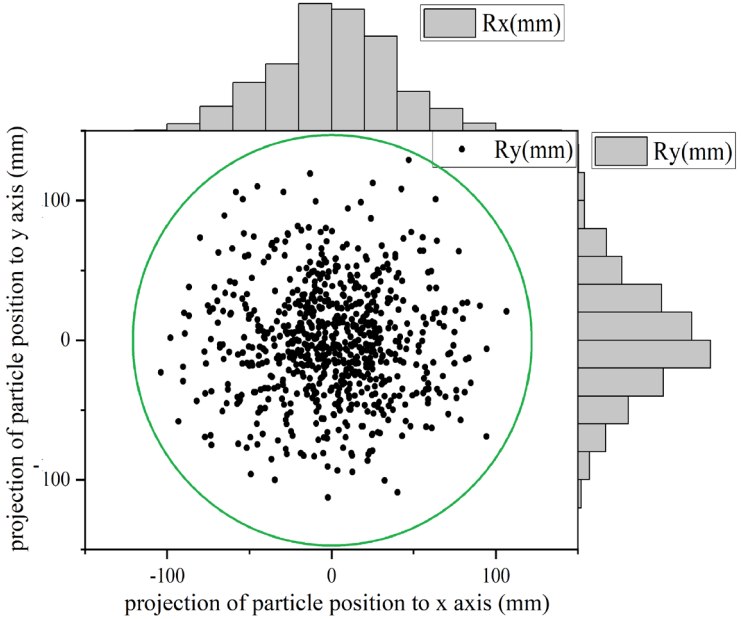


3-dimensional graph for **cloud** of stopped particles (evaporation residua) for isotope $^{182}$Hg, pressure of helium buffer gas 50 mbar and width of entrance window 4 μm, where stopping efficiency is the highest one.

# Simulation of Stopping Efficiency for $^{40}Ar+^{144}Sm \rightarrow {}^{184\text{-}xn}Hg$

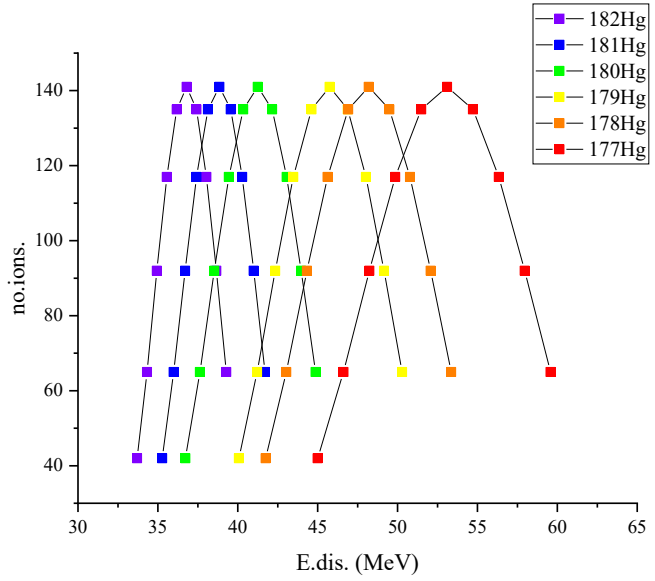


Energy distribution of mercury isotopes of nuclear number 182 to 177.
With decreasing atomic mass number of isotope interval of energy becomes wider and values of energy rises.

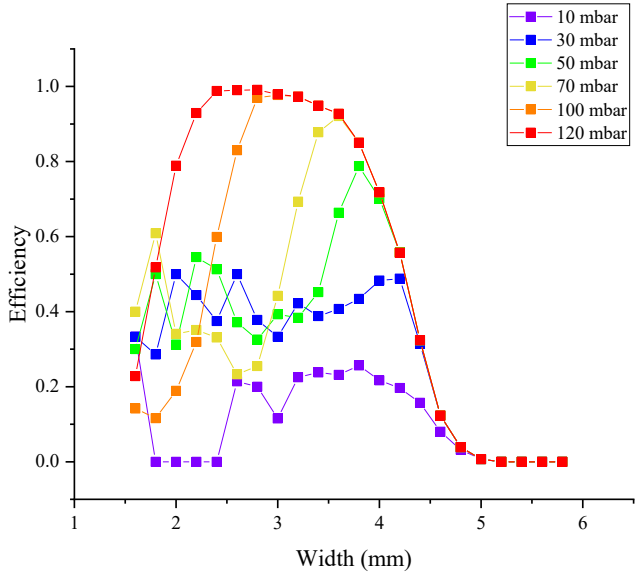


Stopping efficiency dependence on entrance window width and pressure (density) of helium medium for mercury isotopes of nuclear number 179.

This type of graphs is crucial for data analysis. For curve of each pressure peak of stopping efficiency is found and value of efficiency and width of entrance window is wrote down for each of pressures.

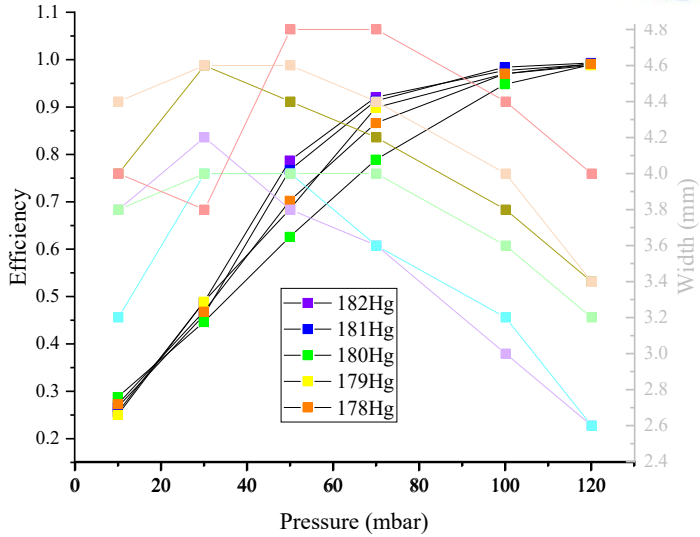


Stopping efficiency dependence on pressure (density) of helium medium (left vertical array) and on entrance window width and pressure (density) of helium medium (right vertical array) for mercury isotopes of nuclear number 182 to 177.

**Right vertical array and horizontal array:**
Entrance window width of maximal stopping efficiency dependence on pressure (density) of helium medium (right vertical array).
Width of maximal efficiency decreases with rising pressure and atomic mass number.
Optimal width and pressure: width from 3.2 to 4.2μm and pressure 50 mbar.

# 5 Time of Flight Simulations

- **2nd part of simulations** (after stopping efficiency)
- **Trajectory of particles** is calculated and graphicaly captured by our **internal software** created in Root framework based on SIMION, Geant4 and COMSOL
- Simulations are based on **file of coordinates** of exact position of stopped particles (it was obtained by previous simulations of stopping efficiency)
- Performed for
  - alpha source $^{220}$**Rn**
  - Isotopes $^{182}$**Hg,** $^{203}$**Rn,** $^{286}$**Fl,** $^{254}$**No**

# Time of flight simulations - example

# $^{182}$Hg, 50 mbar, 4 μm

XYZ_position_file.x...

File Edit Format View Help

```
[PHYSICAL PARAMETERS]
IonZ = 80
AtomicMass = 182.0
Pressure_mbar = 50.0
Temperature = 293.0
Energy_MeV = 36.8
He_density_g_sm3 = 8.208668e-006
Ti_foil_thickness_micro = 4.0

Dist(mm) Rx(mm) Ry(mm)    Useful
--------------------------------
26.5     12.4    14.9    1
115.9    0.1     -34.0    1
0.0      5.5     -12.3    0
0.0      15.4    8.3    0
129.0    9.4     68.7    1
7.2      -4.0    1.4    1
0.0      1.7     -18.4    0
29.8     15.9    7.6    1
0.0      24.2    -4.0    0
0.0      -26.0   5.3    0
41.9     4.6     -34.4    1
71.6     -13.2   -17.1    1
22.6     -17.3   29.5    1
0.0      24.7    -6.3    0
0.0      -10.8   16.3    0
0.0      -10.6   16.3    0
179.3    5.4     40.4    1
113.9    -60.4   65.6    1
0.0      -14.2   -2.8    0
105.4    -0.6    -36.1    1
```

100% Windows (CRLF) UTF-8

GasCellDynamic

**Gas**

Gas amu: 4

Gas Pressure ( mbar: 50

Gas Pressure ( Pa ): 5000.0

Gas Pressure ( Torr ): 37.5

Gas Temperature ( K ): 293

Use Gas Flux (p=1,10,30,50,70 mbar) — View

**Ion**

Ion amu: 182

Ion charge: 1

Energy ( eV ): 100000

Start position X( mm: 50

Start position R ( mm: 0

**Track and field graphics**

X-R track

Z-Y track — Construction

X-Y track

AllTrackDraw

**Electric field**

Use E Field

Use RF

RF amplitude ( V ): 85

RF frequency ( MHz ): 1

U — Change U

Electrode U: 0

Er — Ez--->

RF Er — RF Ez--->

**Run**

Amount of ions: 731

TOF Histo: 132

Run — Stop

Run File

**Ion - Gas collision cross-section**

Gas vdWaals radius ( Angstrom ): 1.4

Ion vdWaals radius (Angstrom ): 2.2

Collision cross-section ( Angstrom^2 ): 40.72

3.14* ( r_vdW_Gas + r_vdW_Ion )^2

```
TOF =  19.57 ms  P=  50.0 mbar T= 293 K  CS= 4.07e-019 m2  E= 0 eV  Xstart = 7 mm  TOF= 19567.8250 ◆s  Run time= 1641.43 (s)
TOF =  21.23 ms  P=  50.0 mbar T= 293 K  CS= 4.07e-019 m2  E= 0 eV  Xstart = 179 mm  TOF= 21228.9427 ◆s  Run time= 1895.10 (s)
TOF =  21.56 ms  P=  50.0 mbar T= 293 K  CS= 4.07e-019 m2  E= 0 eV  Xstart = 116 mm  TOF= 21561.9321 ◆s  Run time= 1948.82 (s)
TOF =  22.36 ms  P=  50.0 mbar T= 293 K  CS= 4.07e-019 m2  E= 0 eV  Xstart = 27 mm  TOF= 22357.9910 ◆s  Run time= 2110.73 (s)
TOF =  22.45 ms  P=  50.0 mbar T= 293 K  CS= 4.07e-019 m2  E= 0 eV  Xstart = 72 mm  TOF= 22448.9777 ◆s  Run time= 2172.70 (s)
TOF =  23.07 ms  P=  50.0 mbar T= 293 K  CS= 4.07e-019 m2  E= 0 eV  Xstart = 30 mm  TOF= 23073.9122 ◆s  Run time= 2233.78 (s)
TOF =  23.87 ms  P=  50.0 mbar T= 293 K  CS= 4.07e-019 m2  E= 0 eV  Xstart = 23 mm  TOF= 23870.9233 ◆s  Run time= 2359.52 (s)
TOF =  25.84 ms  P=  50.0 mbar T= 293 K  CS= 4.07e-019 m2  E= 0 eV  Xstart = 42 mm  TOF= 25843.9658 ◆s  Run time= 2480.67 (s)
TOF =  28.50 ms  P=  50.0 mbar T= 293 K  CS= 4.07e-019 m2  E= 0 eV  Xstart = 129 mm  TOF= 28499.9354 ◆s  Run time= 2658.84 (s)
TOF =  34.09 ms  P=  50.0 mbar T= 293 K  CS= 4.07e-019 m2  E= 0 eV  Xstart = 114 mm  TOF= 34094.0371 ◆s  Run time= 3081.87 (s)
TOF =  23.27 ms  P=  50.0 mbar T= 293 K  CS= 4.07e-019 m2  E= 0 eV  Xstart = 105 mm  TOF= 23274.8559 ◆s  Run time= 1921.75 (s)
```

Trace — Calculation speed 1/min: 0.05 — Threads: 10 — Steps per mean free path: 20 — Cancel

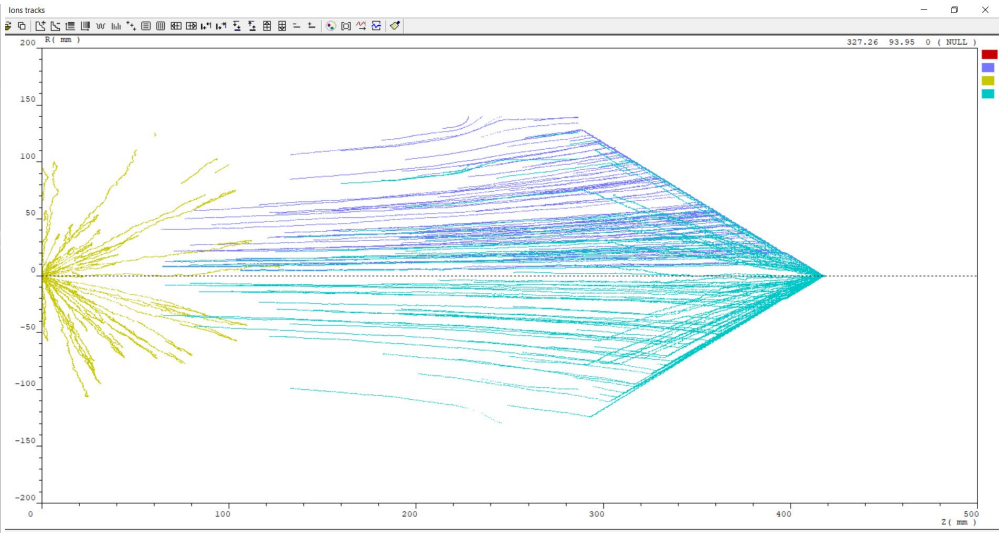

# Alpha source $^{220}$Rn – TOF, dispersion

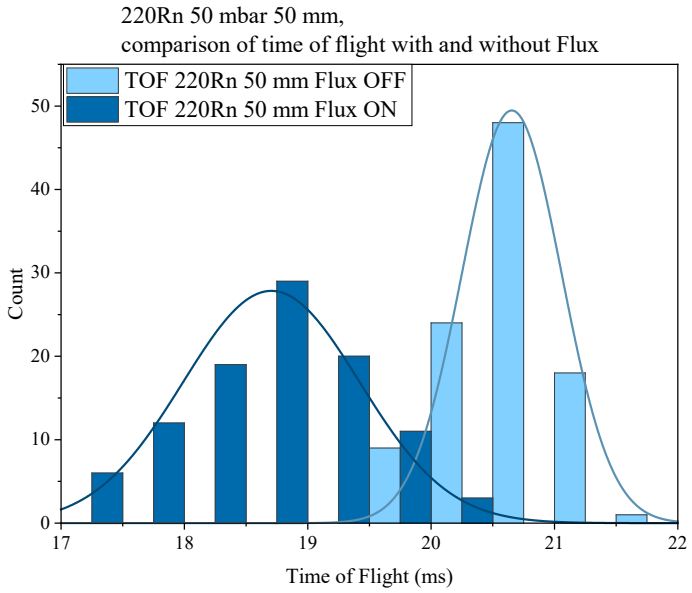


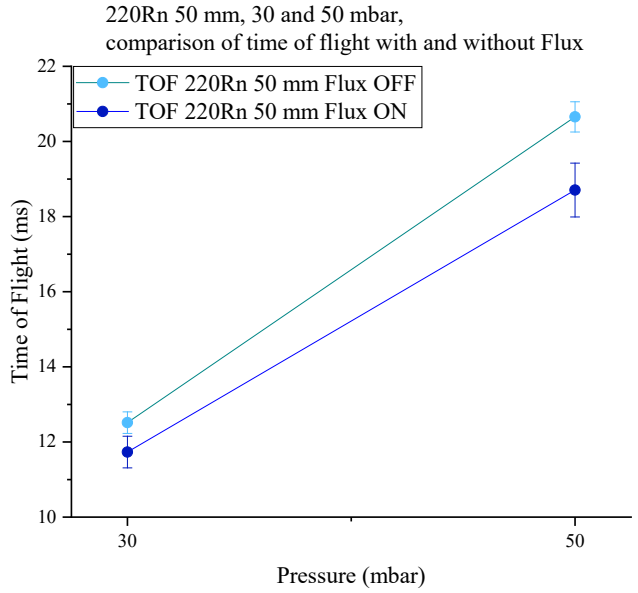


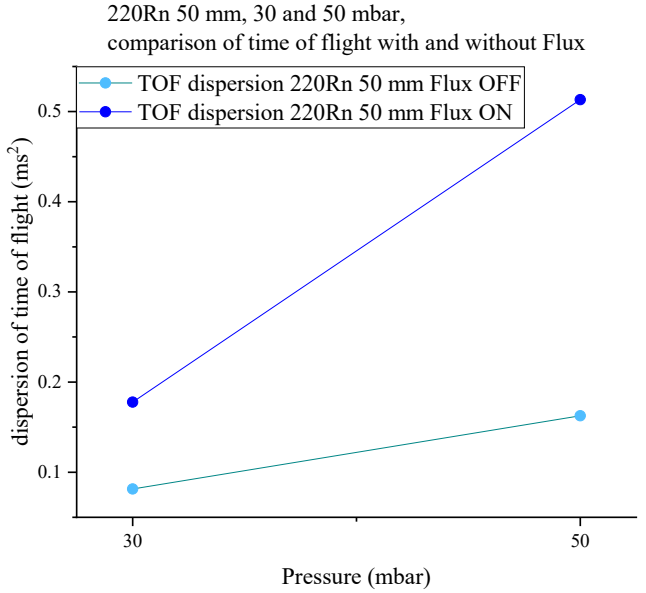


| | TOF Mean value (ms) | SD (ms) | dispersion (ms²) |
|---|---|---|---|
| 30 mbar Flux OFF | 12.51453404 | 0.285378688 | 0.081440995 |
| 30 mbar Flux ON | 11.73141236 | 0.421594288 | 0.177742 |
| 50 mbar Flux OFF | 20.65389362 | 0.403213911 | 0.162581 |
| 50 mbar Flux ON | 18.70496449 | 0.716435218 | 0.513279 |

| Pressure (mbar) | TOF Flux OFF (ms) | SD of TOF Flux OFF (ms) | TOF Flux ON (ms) | SD of TOF Flux ON (ms) |
|---|---|---|---|---|
| 30 | 12.51453 | 0.28538 | 11.73141 | 0.42159 |
| 50 | 20.65389 | 0.40321 | 18.70496 | 0.71644 |

| Pressure (mbar) | TOF dispersion Flux OFF (ms²) | TOF dispersion Flux ON (ms²) |
|---|---|---|
| 30 | 0.08144 | 0.17774 |
| 50 | 0.16258 | 0.51328 |

# 6 Results

## $^{182}$Hg, 2*n* chanel of $^{40}$Ar+$^{144}$Sm→$^{184}$Hg* pressure 30 mbar, comparison of GasCellDynamic without and with Flux function

### 3 µm

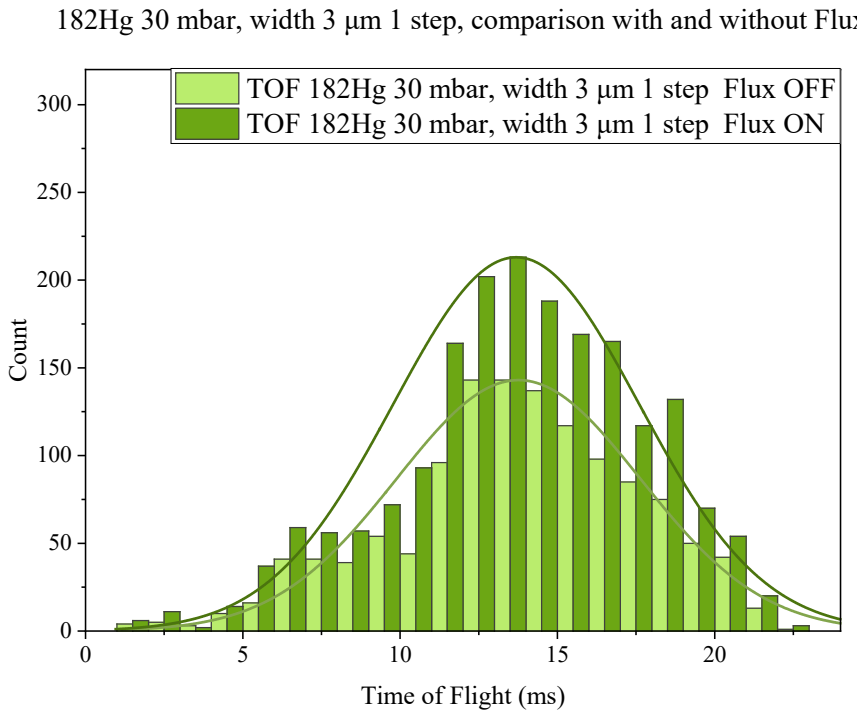


### 4 µm

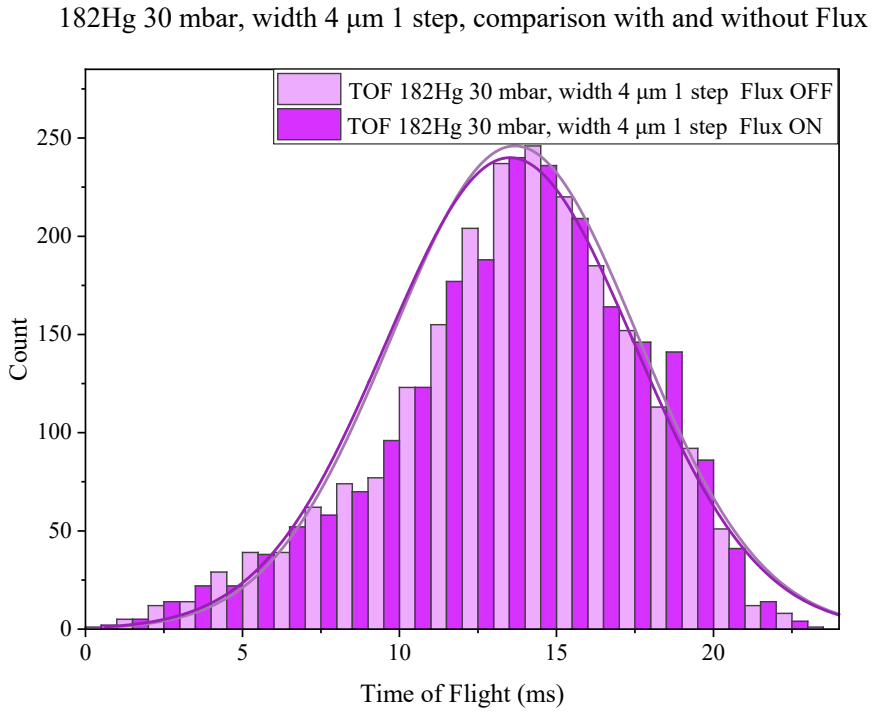


| | TOF Mean value (ms) | SD (ms) | dispersion (ms$^2$) |
|---|---|---|---|
| 30 mbar 3 µm Flux OFF | 13.76312649 | 3.877259072 | 15.03313791 |
| 30 mbar 3 µm Flux ON | 13.69028361 | 3.913051987 | 15.31197585 |
| 30 mbar 4 µm Flux OFF | 14.31988954 | 3.09997614 | 9.609852068 |
| 30 mbar 4 µm Flux ON | 13.52015829 | 3.955024511 | 15.64221889 |

# $^{182}$Hg, 2*n* chanel of $^{40}$Ar+$^{144}$Sm→$^{184}$Hg* 30 mbar, 50 mbar and 70 mbar comparison of GasCellDynamic without and with Flux function 3 µm

## TOF

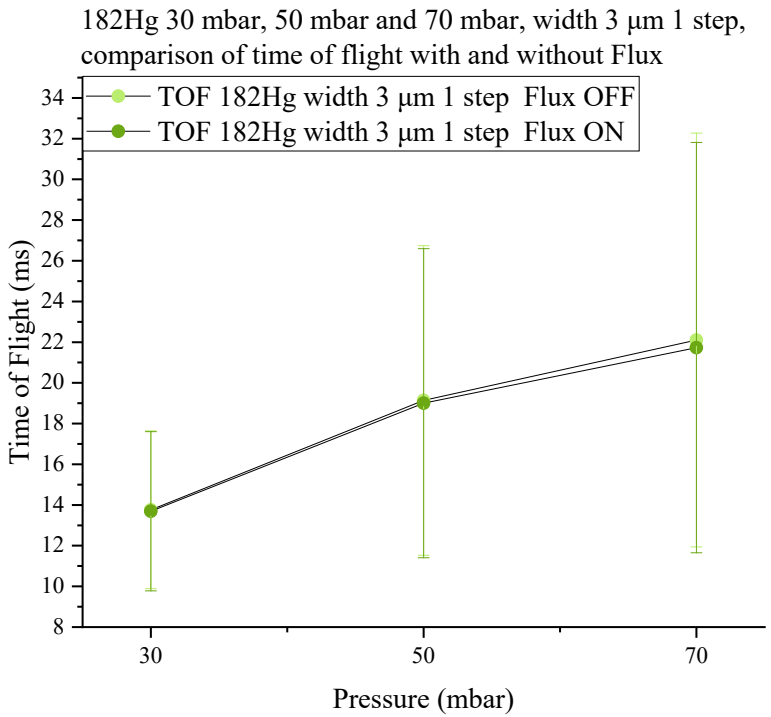


## TOF dispersion

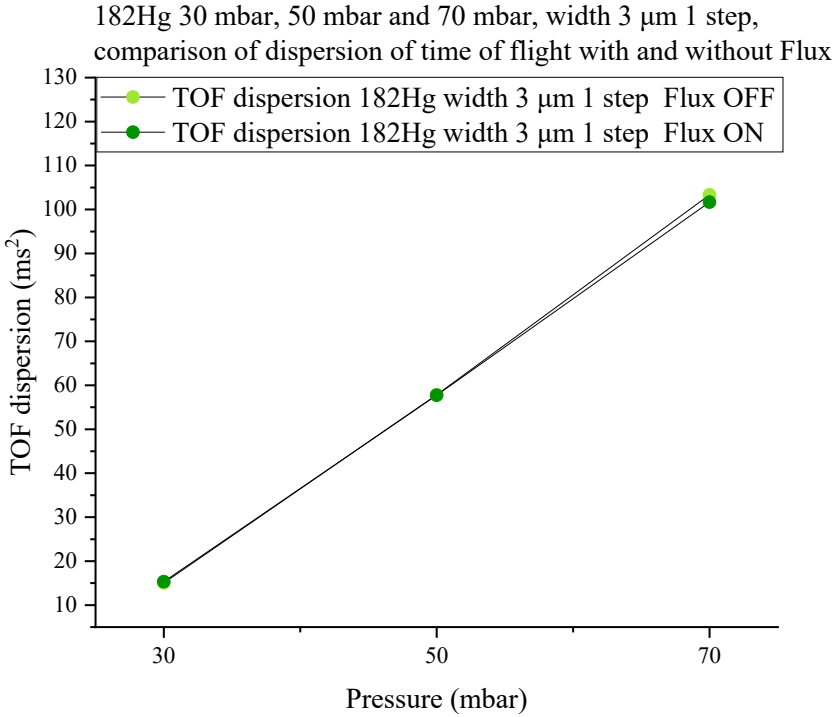


| Pressure (mbar) | TOF Flux OFF (ms) | SD of TOF Flux OFF (ms) | TOF Flux ON (ms) | SD of TOF Flux ON (ms) |
|---|---|---|---|---|
| 30 | 13.76313 | 3.87726 | 13.69028 | 3.91305 |
| 50 | 19.13748 | 7.60531 | 19.00197 | 7.59777 |
| 70 | 22.10447439 | 10.16580165 | 21.73113636 | 10.08250096 |

| Pressure (mbar) | TOF dispersion Flux OFF (ms²) | TOF dispersion Flux ON (ms²) |
|---|---|---|
| 30 | 15.03313791 | 15.31197585 |
| 50 | 57.84081277 | 57.72603467 |
| 70 | 103.3435233 | 101.6568256 |

# 7 Conclusion

- Stopping efficiency - **relies on simulations**, **internal software** in root framework, based on SRIM
- **Reason of simulations** – finding reactions, width of entrance window and pressure of buffer-gas optimal for real experiment (precious and expensive experimental time)
- **Time of Flight - relies on simulations**, software in root framework, based on SIMION, Geant4 and COMSOL
- **Average value** of TOF increases with decreasing value of distance of alpha source (distance from entrance window in direction towards extraction nozzle)
- Average value of TOF decreases with rising gradient on conic electrodes
- Active **Gas Flux function** (is ON) results in decrease of average value of TOF
- Difference between TOF values increases with rise of pressure value
- This observation is in good agreement with theory, **gas dynamics** effects are stronger for higher values of gas pressure.
- **Dispersion** of TOF is higher for activated Gas Flux function than for nonactivated Gas Flux function.
- Values of dispersion of TOF decrease with rising of values of gradient.

# Thank you for your attention.

# Introduction

- Ph.D. Student of Applied physics, Palacky University Olomouc, Czech Republic
- Fifth year
- Supervisor: assoc. prof. Jiří Pechoušek, Ph.D.
- Joint Institute for Nuclear Research in Dubna, Russia
- Flerov Laboratory
- From February 2020
- Consultant: Mgr. Ľuboš Krupa, Ph.D.
- Head of sector: Aleksandr Mikhailovich Rodin, CSc.
- Thesis theme: **Properties of heavy and super heavy elements studied by mass spectroscopy and ISOL method, Stopping Efficiency Simulation of Cryogenic Gas Stopping Cell**

- **Mass**
  - fundamental property of an atom
  - information - its constituents and their interactions, internal structure of the nucleus
  - energy available for nuclear transformations in radioactive decay processes.
- **high-precision mass measurement** (HPMM) of heavy and super heavy elements, a new experimental setup is being built
- The **setup - parts**: target unit; gas-filled separator of complete fusion reaction products; cryogenic gas stopping cell (CGSC); a radio-frequency system for transporting and cooling a low-energy beam; and a multi-reflection time of flight mass spectrometer (MR-TOF MS).
- **CGSC** - final slowing down and thermalizing the energy-bunched fragments produced and selected in the Gas Filled Separator thermalization - in a volume filled with ultra-pure helium gas at cryogenic temperatures.
- After thermalization - fragments are **extracted and transported** with a radio frequency quadrupole (RFQ) to the MR-TOF MS.
- The **stopping and thermalization** of the incoming fusion-evaporation residuals (EVRs) - **key** step in HPMM of the heaviest elements. CGSC has to be as efficient as possible (due to the typically low incoming ion rates and low particle integrals).
- Only the ions that are stopped within the active gas volume of the CGSC can be extracted. The stopping efficiencies for EVRs cannot be tested on-line and one have to rely on simulations. To use the CGSC on ion beam the optimal entrance window foil thickness for every reaction is necessary evaluate.
- **SRIM** software was used

# More about fusion process

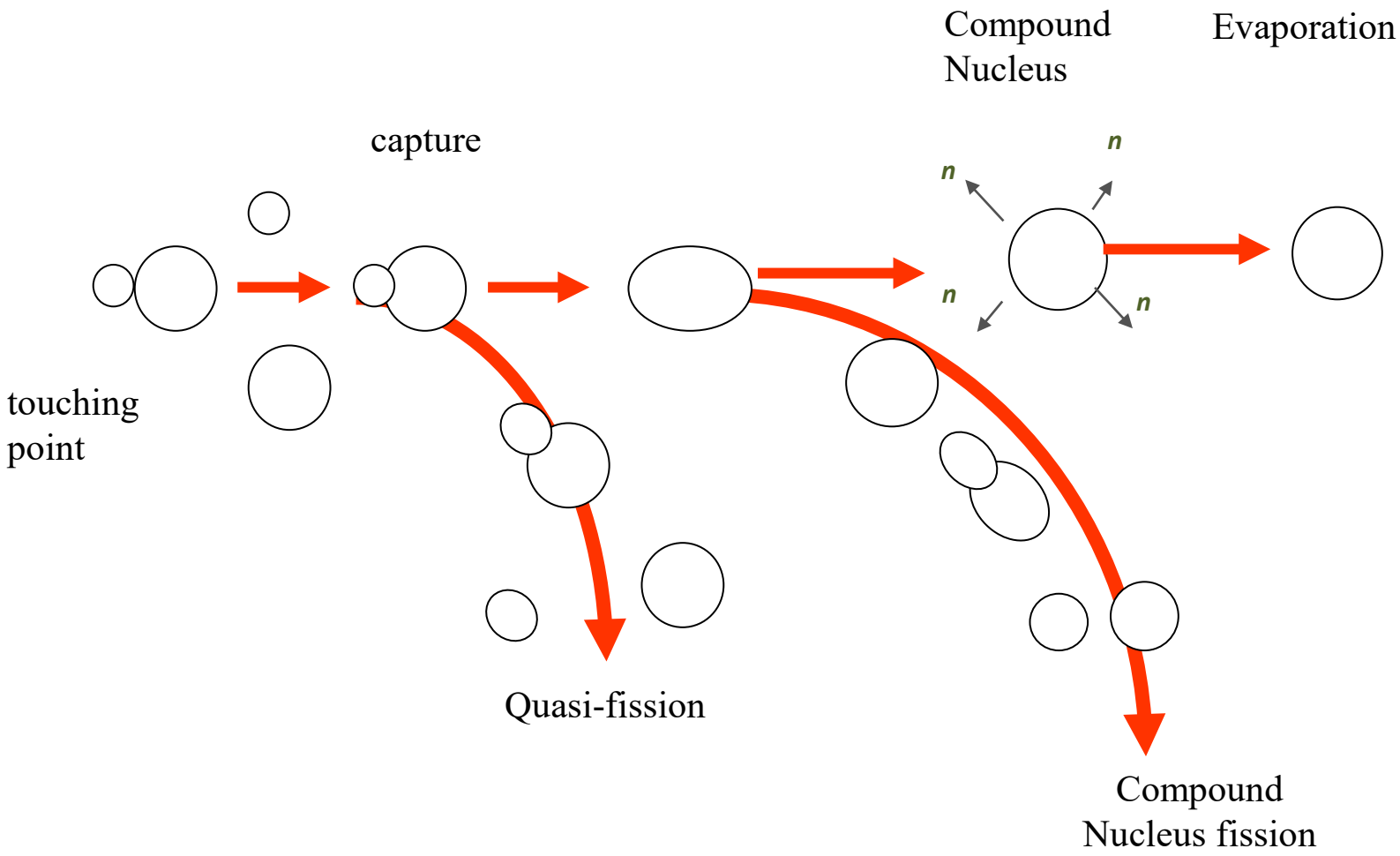


During collision of two nuclei, two cases can happen. Heavier nucleus can capture the lighter one or there can be quasi-fission. After quasi-fission two new nuclei with two new masses are created. In case of capture, one heavier nucleus is created. There are two possibilities again, compound nucleus evaporates neutrons or compound nucleus fissions. After compound nucleus fission, two nuclei of new elements are created. In case of evaporation of compound nucleus, neutron or neutrons are evaporated. As a result, we obtain another isotope of element, not new elements like after compound nucleus fission.

# Periodic Table of the Elements

| | 1 | 2 | 3 | 4 | 5 | 6 | 7 | 8 | 9 | 10 | 11 | 12 | 13 | 14 | 15 | 16 | 17 | 18 |
|---|---|---|---|---|---|---|---|---|---|---|---|---|---|---|---|---|---|---|
| 1 | 1 H Hydrogen 1.008 | | | | | | | | | | | | | | | | | 2 He Helium 4.003 |
| 2 | 3 Li Lithium 6.941 | 4 Be Beryllium 9.012 | | | | | | | | | | | 5 B Boron 10.811 | 6 C Carbon 12.011 | 7 N Nitrogen 14.007 | 8 O Oxygen 15.999 | 9 F Fluorine 18.998 | 10 Ne Neon 20.180 |
| 3 | 11 Na Sodium 22.990 | 12 Mg Magnesium 24.305 | | | | | | | | | | | 13 Al Aluminum 26.982 | 14 Si Silicon 28.086 | 15 P Phosphorus 30.974 | 16 S Sulfur 32.066 | 17 Cl Chlorine 35.453 | 18 Ar Argon 39.948 |
| 4 | 19 K Potassium 39.098 | 20 Ca Calcium 40.078 | 21 Sc Scandium 44.956 | 22 Ti Titanium 47.867 | 23 V Vanadium 50.942 | 24 Cr Chromium 51.996 | 25 Mn Manganese 54.938 | 26 Fe Iron 55.845 | 27 Co Cobalt 58.933 | 28 Ni Nickel 58.693 | 29 Cu Copper 63.546 | 30 Zn Zinc 65.38 | 31 Ga Gallium 69.723 | 32 Ge Germanium 72.631 | 33 As Arsenic 74.922 | 34 Se Selenium 78.971 | 35 Br Bromine 79.904 | 36 Kr Krypton 83.798 |
| 5 | 37 Rb Rubidium 85.468 | 38 Sr Strontium 87.62 | 39 Y Yttrium 88.906 | 40 Zr Zirconium 91.224 | 41 Nb Niobium 92.906 | 42 Mo Molybdenum 95.95 | 43 Tc Technetium 98.907 | 44 Ru Ruthenium 101.07 | 45 Rh Rhodium 102.906 | 46 Pd Palladium 106.42 | 47 Ag Silver 107.868 | 48 Cd Cadmium 112.414 | 49 In Indium 114.818 | 50 Sn Tin 118.711 | 51 Sb Antimony 121.760 | 52 Te Tellurium 127.6 | 53 I Iodine 126.904 | 54 Xe Xenon 131.293 |
| 6 | 55 Cs Cesium 132.905 | 56 Ba Barium 137.328 | 57-71 | 72 Hf Hafnium 178.49 | 73 Ta Tantalum 180.948 | 74 W Tungsten 183.84 | 75 Re Rhenium 186.207 | 76 Os Osmium 190.23 | 77 Ir Iridium 192.217 | 78 Pt Platinum 195.085 | 79 Au Gold 196.967 | 80 Hg Mercury 200.592 | 81 Tl Thallium 204.383 | 82 Pb Lead 207.2 | 83 Bi Bismuth 208.980 | 84 Po Polonium [208.982] | 85 At Astatine 209.987 | 86 Rn Radon 222.018 |
| 7 | 87 Fr Francium 223.020 | 88 Ra Radium 226.025 | 89-103 | 104 Rf Rutherfordium [261] | 105 Db Dubnium [262] | 106 Sg Seaborgium [266] | 107 Bh Bohrium [264] | 108 Hs Hassium [269] | 109 Mt Meitnerium [278] | 110 Ds Darmstadtium [281] | 111 Rg Roentgenium [280] | 112 Cn Copernicium [285] | 113 Nh Nihonium [286] | 114 Fl Flerovium [289] | 115 Mc Moscovium [289] | 116 Lv Livermorium [293] | 117 Ts Tennessine [294] | 118 Og Oganesson [294] |

Number
Symbol
Name
Mass

| | | | | | | | | | | | | | | |
|---|---|---|---|---|---|---|---|---|---|---|---|---|---|---|
| Lanthanide Series | 57 La Lanthanum 138.905 | 58 Ce Cerium 140.116 | 59 Pr Praseodymium 140.908 | 60 Nd Neodymium 144.243 | 61 Pm Promethium 144.913 | 62 Sm Samarium 150.36 | 63 Eu Europium 151.964 | 64 Gd Gadolinium 157.25 | 65 Tb Terbium 158.925 | 66 Dy Dysprosium 162.500 | 67 Ho Holmium 164.930 | 68 Er Erbium 167.259 | 69 Tm Thulium 168.934 | 70 Yb Ytterbium 173.055 | 71 Lu Lutetium 174.967 |
| Actinide Series | 89 Ac Actinium 227.028 | 90 Th Thorium 232.038 | 91 Pa Protactinium 231.036 | 92 U Uranium 238.029 | 93 Np Neptunium 237.048 | 94 Pu Plutonium 244.064 | 95 Am Americium 243.061 | 96 Cm Curium 247.070 | 97 Bk Berkelium 247.070 | 98 Cf Californium 251.080 | 99 Es Einsteinium [254] | 100 Fm Fermium 257.095 | 101 Md Mendelevium 258.1 | 102 No Nobelium 259.101 | 103 Lr Lawrencium [262] |

Alkali Metal | Alkaline Earth | Transition Metal | Basic Metal | Metalloid | Nonmetal | Halogen | Noble Gas | Lanthanide | Actinide